Inflammation, Vol. 42, No. 5, October 2019 (© 2019)
DOI: 10.1007/s10753-019-01016-y

ORIGINAL ARTICLE

Differential Macrophage Subsets in Muscle Damage Induced by a K49-PLA$_2$ from *Bothrops jararacussu* Venom Modulate the Time Course of the Regeneration Process

Priscila Andrade Ranéia e Silva,[1] Adriana da Costa Neves,[2] Cristiani Baldo da Rocha,[3] Ana Maria Moura-da-Silva,[1] and Eliana L. Faquim-Mauro[1,4,5]

Abstract—*Bothrops* snakes cause around 80% of snakebites in Brazil, with muscle tissue damage as an important consequence, which may cause dysfunction on the affected limb. Bothropstoxin-I (BthTX-I) from *Bothrops jararacussu* is a K49-phospholipase A_2, involved in the injury and envenomation's inflammatory response. Immune system components act in the resolution of tissue damage and regeneration. Thus, macrophages exert a crucial role in the elimination of dead tissue and muscle repair. Here, we studied the cellular influx and presence of classical and alternative macrophages (M1 and M2) during muscle injury induced by BthTX-I and the regeneration process. BthTX-I elicited intense inflammatory response characterized by neutrophil migration, then increased influx of M1 macrophages followed by M2 population that declined, resulting in tissue regeneration. The high expressions of TNF-α and IL6 were changed by increased TGF-β expression after BthTX-I injection, coinciding with the iNOs and arginase expression and the peaks of M1 and M2 macrophages in muscle tissue. A coordinated sequence of PAX7, MyoD, and myogenin expression involved in muscle regenerative process appeared after BthTX-I injection. Together, these results demonstrate a direct correlation between the macrophage subsets, cytokine microenvironment, and the myogenesis process. This information may be useful for new envenomation and muscular dysfunction therapies.

KEY WORDS: bothropstoxin-I (BthTX-I); innate immunity; inflammation; M1/M2 macrophages; muscle regeneration.

INTRODUCTION

Local injury with muscle necrosis elicited by distinct agents leads to an inflammatory response with infiltration of immune cells, mainly neutrophils and macrophages, which are responsible for the phagocytosis of dead cells, damaged skeletal muscle tissue as well as the secretion of cytokines that play a relevant

[1] Immunopathology Laboratory, Butantan Institute, São Paulo, Brazil
[2] Laboratory of Division of Genetics, Butantan Institute, São Paulo, Brazil
[3] Londrina State University, Paraná, Brazil
[4] Department of Immunology, Institute of Biomedical Sciences, University of São Paulo, São Paulo, SP, Brazil
[5] To whom correspondence should be addressed at Department of Immunology, Institute of Biomedical Sciences, University of São Paulo, São Paulo, SP, Brazil. E-mail: eliana.faquim@butantan.gov.br

role in the tissue regeneration [1]. Envenoming by snakebites is considered a public health problem and classified as a tropical neglected disease by the WHO [2, 3]. One of the most important consequences of the envenoming by viper snakes is the local tissue damage. In this sense, the envenomation by viper snakes from the *Bothrops* genus results in a complex local reaction with myonecrosis, hemorrhage, edema, blisters, and inflammation that can evolve to complete tissue regeneration or even in a dysfunction of the affected organ [3–5]. Therefore, the understanding of the tissue damage resultant of the snakebites and the mechanisms involved in the tissue regeneration represent a relevant issue to propose new strategies of treatment.

Bothrops venoms are composed of a rich mixture of enzymes and non-enzymatic components in which predominate proteinases, phospholipase A_2, and C-type lectin-like molecules. Among these components, snake venom metalloproteinases (SVMPs) and phospholipase A_2 (PLA_2) are the main toxins involved in the local tissue injury. However, distinct mechanisms are described for local tissue damage induced by each of these two groups of molecules [6–8].

The envenomation by *Bothrops jararacussu*, as all *Bothrops* venoms, also induces strong local and systemic pathophysiological manifestations. The PLA_2 from the *B. jararacussu* venom are important myotoxic components with degenerative events in muscle cells [9, 10]. The bothropstoxin-I (BthTX-I) isolated from the *B. jararacussu* venom is a lysine-49 phospholipase A_2, non-enzymatically active with molecular weight of 13.7 kDa [11, 12]. BthTX-I promotes myonecrosis, edema, pain, inflammation, cytotoxicity, and neurotoxicity as well as anti-coagulant effect [9–11, 13] contributing to the pathology of the envenomation. The mechanisms of myotoxic K-49 PLA_2s include their binding to acceptors in plasma membrane of target cells resulting in disruption of the membrane integrity. This change in the plasma membrane causes a series of events such as a rapid depolarization with influx of calcium (Ca^+), which triggers hyper myofilament, mitochondrial damage, and activation of proteases and PLA_2 intracellular Ca^+-dependent, which together contribute to the necrotic process [14–17].

In this context, myotoxic PLA_2s are keys in establishing the local tissue damage in the envenomation, and therefore are targets for studies aimed to elucidate its mechanisms of action to improve the envenomation treatment [18, 19].

After the muscular tissue injury, myogenic cells are activated, differentiated into myoblasts, and, after several rounds of replication, merge into multinucleate myotubes that become mature myofibers [20, 21]. The inflammatory reaction is closely associated with the muscular tissue regeneration. As shown in several experimental models, the macrophages develop a crucial role for the appropriate regenerative process [1]. As previously shown, cytokines and microbial products differentially affect the activation and consequent function of the macrophages in the immune response [1, 22, 23]. In this sense, the macrophages have been classified into two subpopulations according to their phenotype and functions [24, 25]. The M1-type macrophages (M1) present a pro-inflammatory profile with strong microbicidal activity, high expression of inducible nitric oxide synthase (iNOS), production of reactive oxygen and nitrogen species, and secretion of TNF-α, IL-8, IL-1β, IL-6, and IFN-γ. These cells are mainly present in the inflammatory phase of the reaction and therefore involved in the elimination of pathogens or tumor cells [23]. In contrast, the alternative M2-type macrophages (M2) show high expression of the arginase enzyme and develop a regulatory role in the immune response, predominantly by secreting IL-4, IL-10, and TGF-β. These M2 cells act in controlling the inflammatory response and promoting angiogenesis, tissue repair, and remodeling [25]. Experimental findings show that in acute muscle injury, the immune response profile is characterized by a dominant pro-inflammatory response mediated by neutrophils and M1 macrophages, which also cause further damage by secretion of cytokines and nitric acid. These cells eliminate the death tissue and stimulate the proliferative phase of myogenesis. Following this inflammatory phase, the presence of M2 macrophages attenuates the M1 population and, through the secretion of anti-inflammatory cytokines, promotes the growth and muscle regeneration. Therefore, as observed in chronic muscle injuries, an imbalance in these kinetics of the immune response may compromise the appropriate regeneration [1, 26–30].

Considering the action of PLA_2s in the muscle injury observed in the *Bothrops* envenomation, here we analyzed the kinetics of the macrophage populations and consequent regeneration process elicited by BthTX-I injection in gastrocnemius muscle of mice. Thus, this study contributes to the understanding of the effect of isolated toxin on the muscle tissue as well as the functional subsets of macrophages that regulate the temporal muscle regeneration process, which can provide relevant information to effective therapeutic

approaches for treating snakebite envenomation and diseases associated with muscular dysfunctions.

MATERIALS AND METHODS

Mice

For the experiments, male mice of BALB/c mice, weighing between 20 and 22 g, were bred from the animal house facilities of the Butantan Institute, São Paulo, Brazil. The animals were maintained under controlled temperature, 12/12 light/dark cycle, and standard food and water *ad libitum*. The experimental protocols were approved by the Butantan Institute Ethical Committee for Animal Research (CEUAIB-879/12 and 1286/14).

B. jararacussu Venom

The venom of *B. jararacussu* was obtained from the pool of venoms extracted from snakes kept in captivity in the central animal facility of the Herpetology Laboratory, Butantan Institute, São Paulo, SP. The BthTX-I was isolated from the whole venom according to Moura-da-Silva [31].

Experimental Groups

Groups of mice ($n = 4$) received in the right gastrocnemius muscle 50 μg of BthTX-I (50 μL/animal) diluted in sterile saline. As a control, one group of mice received 50 μL of sterile saline. Four hours after the toxin injection, four mice from each group were bled to obtain plasmas and detection of creatine kinase levels using the UV kinetic CK (BioClin). Other animal groups received the toxins at different time intervals (4 h, 24, 48, 72, and 96 h, 7 and 28 days) and were euthanized to obtain the muscle region injected with the toxin. This tissue was used for the histological analysis, preparation of cell suspension for analysis of flow cytometry, or RNA extraction for real-time PCR (RT-PCR).

Histological Analysis of Muscle Tissue

A small portion of the gastrocnemius muscle was carefully removed and fixed in 10% formaldehyde in PBS (*v*/*v*) for 24 h at room temperature. Then, the tissues were dehydrated in 100% ethanol and dipped in xylene, and the samples were embedded in Paraplast-Histosec (Merck) resin. Sections of 5-mm thickness were adhered to glass slides previously coated with poly-L-lysine and subsequently used for histochemical procedures, and, finally, stained with hematoxylin-eosin solution for morphological studies of tissues.

Analysis of the Cellular Infiltrate in Muscle Tissue by Flow Cytometry

The cellular migration in the gastrocnemius muscle after different time points of BthTX-I injection was analyzed by flow cytometry. Groups of mice ($n = 4$) were euthanized, and a small portion of the muscle was collected and placed in culture medium (RPMI 1640, Invitrogen) containing 0.02% trypsin followed by incubation for 30 min at 37 °C. After this, the tissues were macerated in sterile homogenizer in culture medium and centrifuged for 5 min at 1200 rpm at 4 °C and the cell pellet re-suspended in RPMI 1640 medium supplemented with 2 mM L-glutamine, 50 μM 2-ME, and 5% fetal bovine serum (FBS) (RPMI-S). The cell count and the viability were performed in a Neubauer chamber using Trypan blue 0.2%. The cell suspensions were incubated with erythrocyte lysis buffer for 1 min at RT, centrifuged (5 min/1200 rpm/4 °C), re-suspended in RPMI medium, and incubated with anti-FcγRII/III for 30 min at 4 °C. Afterwards, the cell suspensions were centrifuged (5 min/1200 rpm/4 °C) and re-suspended in culture medium (10^6 cells/well) followed by incubation with anti-leukocyte antibodies (CD45-APC), anti-neutrophil (Ly6G-PE) and anti-macrophage (F4/80-FITC) or anti-macrophage (F4/80-FITC), anti-CD68 (PE), and anti-CD206 (Alexa-Fluor 488) monoclonal antibodies (BD bioscience) for analysis of M1 and M2 macrophages, respectively, followed by incubation for 30 min at 4 °C. The cell samples were washed and re-suspended in PBS containing 0.1% paraformaldehyde (Merck). All samples were analyzed in the flow cytometer (FACSCanto II, Becton Dickinson). The data were analyzed with FlowJo software 7.5 and expressed as the mean of the cell numbers of individual mice/group ± standard deviation (SD).

Gene Expression by PCR-RT

Cell suspensions prepared from the macerated gastrocnemius muscle were adjusted to a concentration of 1×10^7 and centrifuged for 8 min, 1200 rpm at 4 °C. The supernatants were removed and the cells re-suspended in 1.0 mL of Trizol (Invitrogen) at RNase-free conditions. The cDNA was transcribed from RNA using 200 U/μL of SuperScript III RT (Invitrogen) in the presence of 50 μM Oligo(dT), 10 mM dNTP mix, 5× *first-strand buffer*, 100 mM DTT, and *Rnase OUT* inhibitor (40 U/μL) at 50 °C for 60 min. The reaction was inactivated by warming

to 70 °C for 15 min, and the quantitative RT-PCR was performed using LineGene K Thermal Cycler (Hangzhou Bioer Technology Co.) and the *fqdpcr-4.2.20* software. For this, the reactions were performed using the qPCR-Rox SYBR Green Plus (LGC Biotechnology) kit. Pairs of specific primers for the transcriptions gene (myogenin, Pax-7, MyoD), arginase, iNOS, and cytokines (IL-6, TNF-α, and TGF-β) were designed and synthesized (Thermo Fisher Scientific) specifically for this reaction [32, 33]. Relative quantification of gene expression was performed by comparison with the endogenous β-actin control. For each reaction, it was used 1 μL cDNA (250 ng), 1 μL forward primer and reverse primer (10 μM), 6.5 μL Platinum SYBR, 0.25 μL Rox Dye, and 2.25 μL H_2O. The following thermal cycling protocol was used: 50 °C for 2-min hold (UDG incubation), 95 °C for 2-min hold, followed by 40 cycles of 95 °C, 15 s and 60 °C, 30 s (60 s for the 7900HT). To determine the melting curve of each amplified product, the temperature was decreased from 95 to 65 °C, with a decrease of 0.5 °C every 20 s.

The data were normalized using β-actin as a housekeeping gene and then analyzed by comparative threshold cycle (C_T) method to calculate fold changes of expression in cell suspensions at different time points of toxin injection, where $\Delta C_T = C_T$ of gene of interest minus C_T of β-actin and $\Delta\Delta C_T = \Delta C_T$ of cell suspensions minus ΔC_T of cell suspensions from saline group. Fold changes in gene expression for cell cultures incubated with the different toxins in the presence or not of LPS were then calculated as $2^{\Delta\Delta CT}$. The efficiency for each set of primer was 100%. All real-time experiments were performed in triplicate of three independent cell culture experiments.

Statistical Analysis

Statistical analysis was performed by one-way ANOVA followed by Tukey or Bonferroni test (GraphPad Prism 5.0, GraphPad Software). p values < 0.05 were considered statistically significant. All data were representative of at least two or three independent experiments.

RESULTS

Histological Analysis of Muscle Tissue Injected with BthTX-I

As previously shown, the local tissue injury with muscle necrosis is one of the deleterious effects in the *Bothrops* envenomation. Thus, we evaluated the local injury induced by BthTX-I injection in gastrocnemius muscle and regeneration process. For this, mice received the toxin in gastrocnemius muscle, and after different time points, the tissue damage, cellular infiltration, and fiber regeneration were analyzed in histological sections.

Twenty-four hours after saline injection, control tissues presented normal skeletal muscle without inflammatory infiltrate and necrotic area (Fig. 1a). In contrast, 24 h after BthTX-I injection, we observed large areas of myofiber necrosis, edema, and predominance of neutrophilic inflammatory infiltrate (Fig. 1b). At 48 h after toxin injection, we detected large areas of myofiber necrosis, presence of neutrophils, and scarce macrophages (Fig. 1c). Figure 1d shows few neutrophils present in contrast with large amounts of macrophages near to necrotic muscle fibers as well as the presence of myoblasts, indicating that the repair was initiated at 72-h post-toxin injection (Fig. 1d). Ninety-six hours after BthTX-I injection, there was myoblast proliferation and the beginning of muscle fiber formation. It was still observed large amounts of necrotic muscle fibers and presence of several macrophages (Fig. 1e). Seven days after toxin injection, it was observed the presence of newly formed myofibers centrally nucleated and several macrophages and still multinucleated giant cells phagocyting the debris of necrotic muscle fibers (Fig. 1f). On day 28 post-toxin injection, it was verified few necrotic muscle and inflammatory cells in focal areas (Fig. 1g); however, most of the muscle tissue was already repaired (Fig. 1h).

Inflammatory Cell Profile in Gastrocnemius Muscle Induced by BthTX-I Injection

In order to determine the cellular profile infiltrated in the gastrocnemius muscle after BthTX-I injection, we analyzed the cell populations by flow cytometry. For this, at 4, 24, 48, 72, 96 h, or 7 and 28 days after the BthTX-I injection, the cell suspensions were prepared from the gastrocnemius muscle, stained with different fluorescent monoclonal antibodies followed by flow cytometry analysis.

Figure 2a represents the gate strategy used to analyze the leucocyte infiltration in the gastrocnemius muscle induced by BthTX-I injection. As shown in Fig. 2b, BthTX-I elicited predominant neutrophil ($CD45^+/Ly6G^+$) migration at the initial times evaluated compared with the saline group. Furthermore, higher macrophage ($CD45^+/F4/80^+$) infiltration was observed in the BthTX-I group compared with control group at 48–96 h after the toxin injection (Fig. 2c). No difference in the number of neutrophils and macrophages on

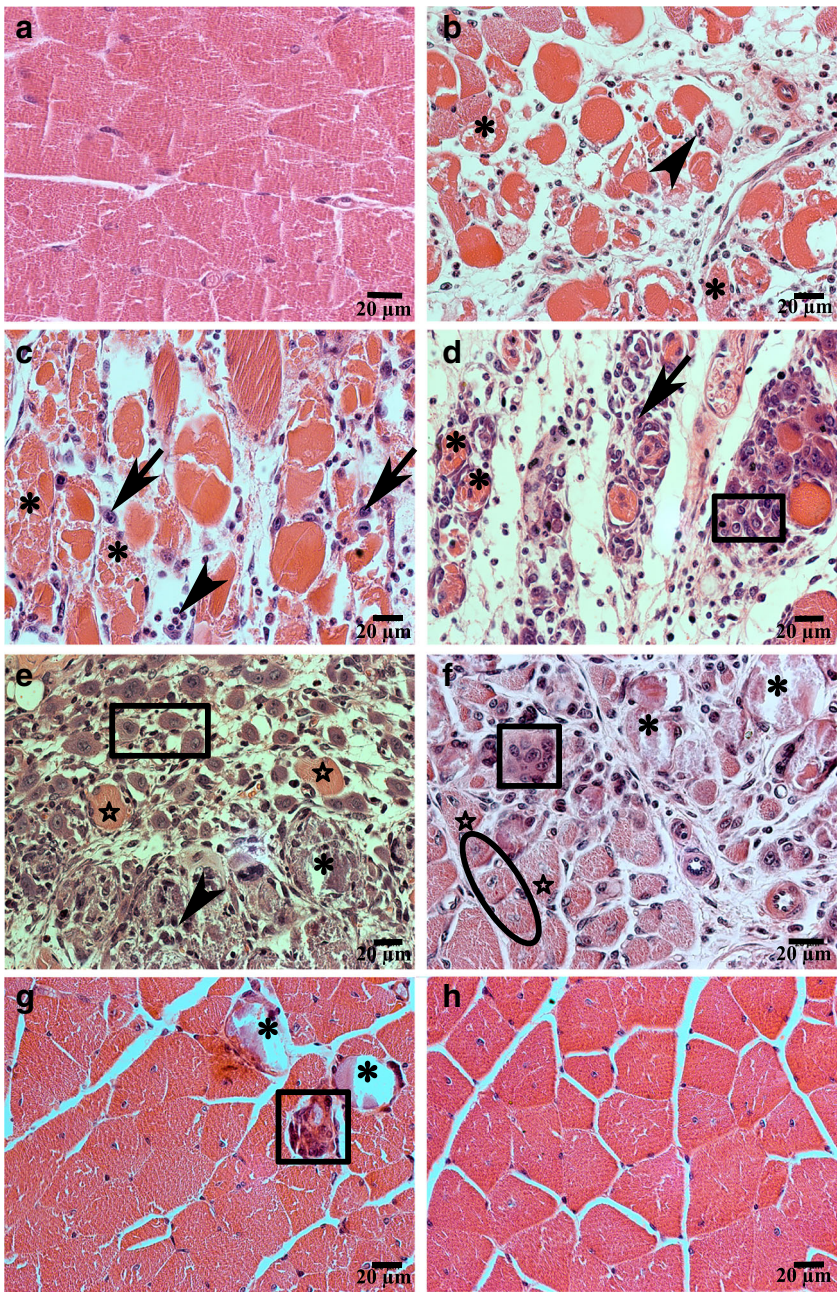

Fig. 1. Muscle histology at different time points of BthTX-I injection. Hematoxylin and eosin staining. **a** Twenty-four hours after saline injection. **b** Twenty-four hours, **c** 48 h, **d** 72 h, **e** 96 h, **f** 7 days, and **g**, **h** 28 days after BthTX-I injection in gastrocnemius muscle. Myonecrosis (asterisk), neutrophilic inflammatory infiltrate (arrowhead), macrophages (black arrow), myoblasts (rectangle), myofibers (stars), myofibers with central nuclei (oval shape), multinucleated giant cells (square). The images are representative of three to four mice/group. Bar 20 μm.

gastrocnemius muscle was observed between the BthTX-I group and saline group at 28 days. Therefore, the data demonstrate a sequential migration of neutrophils and macrophages in the muscle tissue over the time of the toxin injection.

Evaluation of M1 and M2 Macrophages in the Gastrocnemius Muscle After BthTX-I Injection

As mentioned, macrophages with distinct phenotypes (M1 and M2) play different roles in the inflammatory

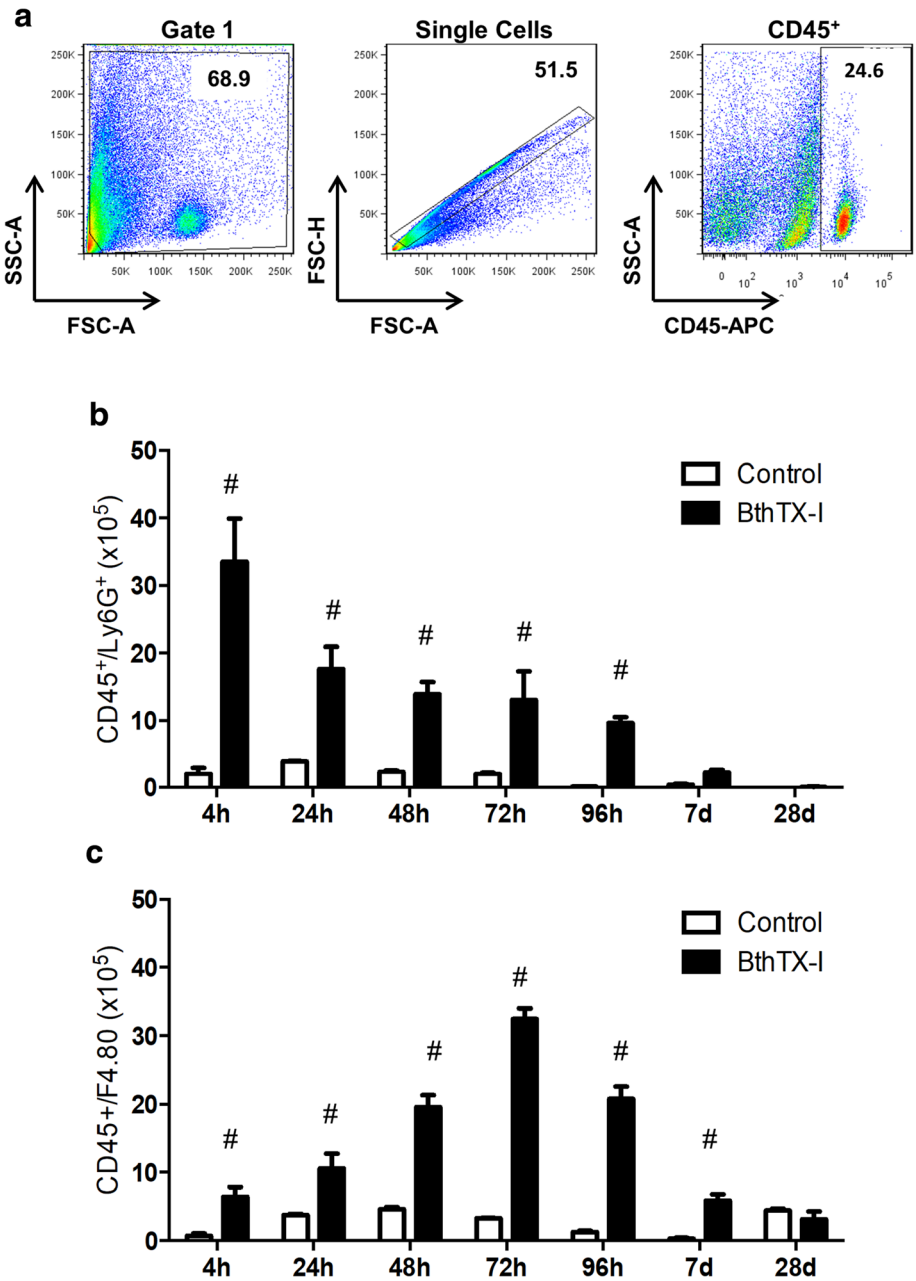

Fig. 2. Kinetics of leukocyte migration in gastrocnemius muscle of BALB/c mice injected with BthTX-I. Cell suspensions were prepared from muscle macerates after 4, 24, 48, 72, 96 h, 7, 14, and 28 days of the injection of BthTX-I (50 μg) in gastrocnemius muscle. The control group was injected with sterile saline. All samples were analyzed by flow cytometry. The data represent the mean of the absolute number of the positively labeled cells of the individual animal ($n = 4$)/group ± SD. **a** Gate strategy used in the experiment, with exclusion of doublet cells. **b** Absolute number of positively labeled cells in suspensions obtained from the different experimental groups (1×10^6 cells) and incubated with anti-leukocytes (CD45-APC) and anti-Ly6G (PE) antibodies. **c** Number of double-labeled cells in suspensions obtained from the different experimental stained with anti-CD45 (APC) and anti-F4/80 (FITC) antibodies. Statistical analysis was performed by ANOVA, followed by the Bonferroni test. #$p < 0.05$ BthTX-I group compared with control group.

response and tissue regeneration [1, 27, 34]. Thus, we analyzed the M1 ($F4/80^+/CD68^+$) and M2 ($F4/80^+/CD206^+$) macrophage profile in response to the injection of the toxin, by flow cytometry. In addition, we analyzed—by real-time PCR—the expression of iNOS as an indicator of M1 and

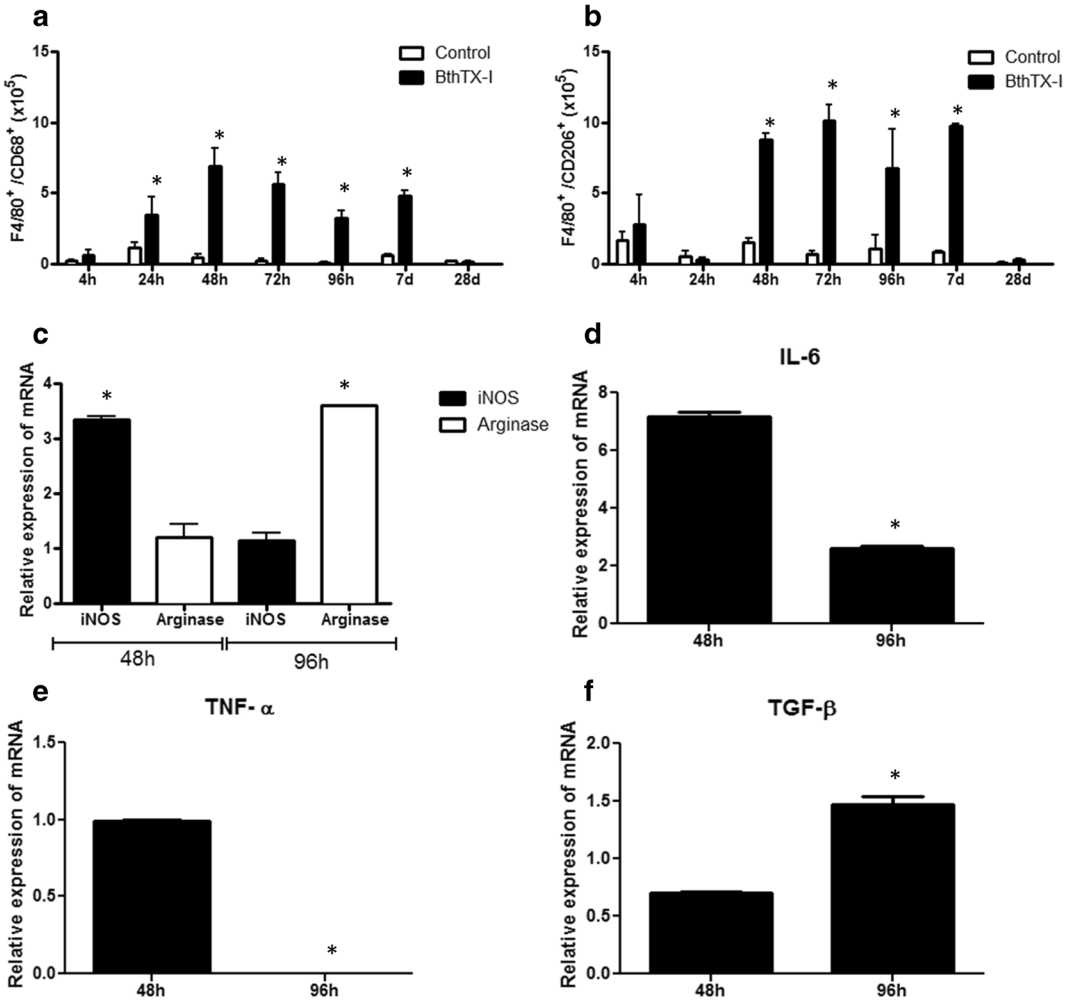

Fig. 3. Phenotypes of macrophages and gene expression of iNOS, arginase, IL-6, TNF-α, and TGF-β in gastrocnemius muscle of BALB/c mice injected with BthTX-I. Cell suspensions were prepared from macerate muscle after 4, 24, 48, 72, 96 h, 7, and 28 days of injection of BThTX-I (50 μg) in gastrocnemius muscle. The control group was injected with sterile saline. All samples were analyzed by flow cytometry. The data represent the mean of the absolute number of the positively labeled cells of the individual animal ($n = 4$)/group ± SD. **a** Absolute number of cells positively labeled with anti-F4/80 and anti-CD68. **b** Absolute number of cells positively labeled with anti-F4/80 and anti-CD206. Statistical analysis was performed using the ANOVA test (followed by the Bonferroni test). *$p < 0.05$ BthTX-I group compared with control group. **c** Relative gene expression of iNOs and arginase in the muscle macerate of individual BALB/c mice injected with BthTX-I ($n = 4$) ± SD; the β-actin gene expression was used as constitutive gene control. *$p < 0.05$ arginase expression compared with iNOS expression in macerate muscle of BthTX-I-injected mice. **d** Gene expression of IL-6, **e** TNF-α, and **f** TGF-β in the macerate muscle of BALB/c mice injected with BthTX-I ($n = 4$) ± SD. *$p < 0.05$. Samples of macerate muscle of 48 h compared with 96 h of BthTX-I-injected mice.

arginase for M2 macrophages in cell suspensions prepared from the site of the toxin injection [25, 35].

The results in Fig. 3a show a peak of M1 macrophages at 48—72 h after BthTX-I injection compared with the control group. In addition, the expression of iNOs by the cell suspension was higher at 48 h after the BthTX-I injection compared with the arginase expression (Fig. 3c).

The results also show higher number of M2 macrophages after 48 h remaining elevated up to 7 days after the toxin injection in comparison with saline group (Fig. 3b). Furthermore, increased expression of arginase was detected in cell suspension after 96 h of BthTX-I injection in comparison with iNOS expression (Fig. 3d). The data also demonstrate a predominant expression of IL-6 and TNF-α in cell suspension of mice injected with BthTX-I at 48 h compared with the TGF-β expression. In contrast, at 96 h after the toxin injection, the expression of pro-

inflammatory cytokines was downregulated in comparison with the increased expression of TGF-β (Fig. 3d–f).

Evaluation of Gene Expression Involved in Muscle Repair and Regeneration

After an injury, sequential events are developed for the appropriate muscle regeneration including the expression of transcription factors that regulate the myogenesis and generation of new fibers [36–38]. In this sense, we analyzed the Pax-7 expression as a marker of myogenic satellite cells [39] and the transcription factors MyoD and myogenin that are activated during the muscle regeneration process after the BthTX-I injection.

Figure 4a shows high expression of Pax-7 in cell suspensions obtained after 4 h of the BthTX-I injection. The expression of PAX-7 was also increased on day 28, suggesting the presence of satellite cells in freshly regenerating muscle tissue in the BthTX-I group.

The expression of RNAm for MyOD that regulates the proliferation and differentiation of the muscle cells [40] was also analyzed, and the results show increased expression of this factor in cell suspensions obtained after 48–72 h of the toxin injection (Fig. 4b).

As verified in Fig. 4c, the expression of myogenin, which is important for the fusion process of myotubes [41], was enhanced at 72 h after the toxin injection and remaining for up to 28 days in BthTX-I group.

DISCUSSION

Several studies have highlighted the relevant role of PLA_2s in the local pathology observed in envenomation [9–11, 13, 42–45]. It is known that innate immune cells participate in both the local inflammatory reaction and muscle regeneration [46]. However, the correlation between the local damage induced by snake toxins and the appropriate tissue regeneration is not completely clarified. In this context, here we demonstrate the close relationship between the coordinated predominance of subsets of macrophage (M1 and M2), cytokine microenvironment, and the time course of the myogenesis in an injured muscle by the K49-PLA_2 myotoxin injection.

Studies on the cellular infiltrate kinetics in acute muscle lesions show that neutrophils are the first inflammatory cells to reach the lesion site. These cells release MPO, cytokines, bradykinin, prostaglandin, and histamine causing vasodilation and increased permeability of small vessels and migration of other cells to the tissue local. The neutrophil infiltration decreases after about 2 days followed by the macrophage influx. Thus, macrophages presenting different phenotypes also participate in this phase as well as in subsequent steps modulating cell proliferation and tissue repair processes [1].

Particularly, the injection of carrageenan (Cg), as a pro-inflammatory agent, induces skeletal muscle inflammation *in vivo* similar to that seen in exercise muscle damage, and therefore has been strongly used to evaluate the relationship between inflammatory response and pain [47–50]. The inflammation induced by Cg is characterized by accumulated neutrophils in the perivascular space followed by the presence of macrophages, which are accompanied by the local release of soluble molecules, such as cytokines and lipid mediators, which contribute for hyperalgesia and/or weakness [51]. However, in these studies, the subsets of macrophages and their relevance for the pain observed after the Cg injection were not evaluated.

In addition, currently, muscle injury provoked by myotoxic toxins, chemical agents, and physical procedures has been also used to study the mechanisms involved in the muscle regeneration. Despite the fact that all of them started with severe necrosis, differences in the intensity and kinetics of the tissue repair have been reported [52]. In this context, Hardy and collaborators compared the regenerative process with muscle injury induced by (a) freezing (FI) or (b) or injection of barium chloride ($BaCL_2$), notexin (NTX, a PLA_2 neurotoxin), and cardiotoxin (CTX, PKC-specific inhibitor). The authors described that the initial phase is critical for the regeneration outcome; however, all of them restored the muscle tissue. Furthermore, they verified that, differently from the FI model, the intramuscular injection of CTX, NTX, and $BaCL_2$ provoked a monophasic necrosis followed by the sequential infiltration of neutrophils and macrophages. Although the kinetics appeared to be identical, differences in the production of cytokines were observed, as well as the regeneration kinetics. Therefore, the authors' data indicate that, despite of all compounds being able to induce an initial inflammation, the biological activity of the molecule should be considered such as the toxins themselves, which not only injure the muscle but might also affect inflammatory cells and consequent tissue repair.

Our data of flow cytometry confirm the histological findings of early neutrophilic infiltration followed by macrophage presence after the BthTX-I injection simultaneously to the necrosis of muscle fibers and release of creatine kinase (CK), which are consequences of the potent

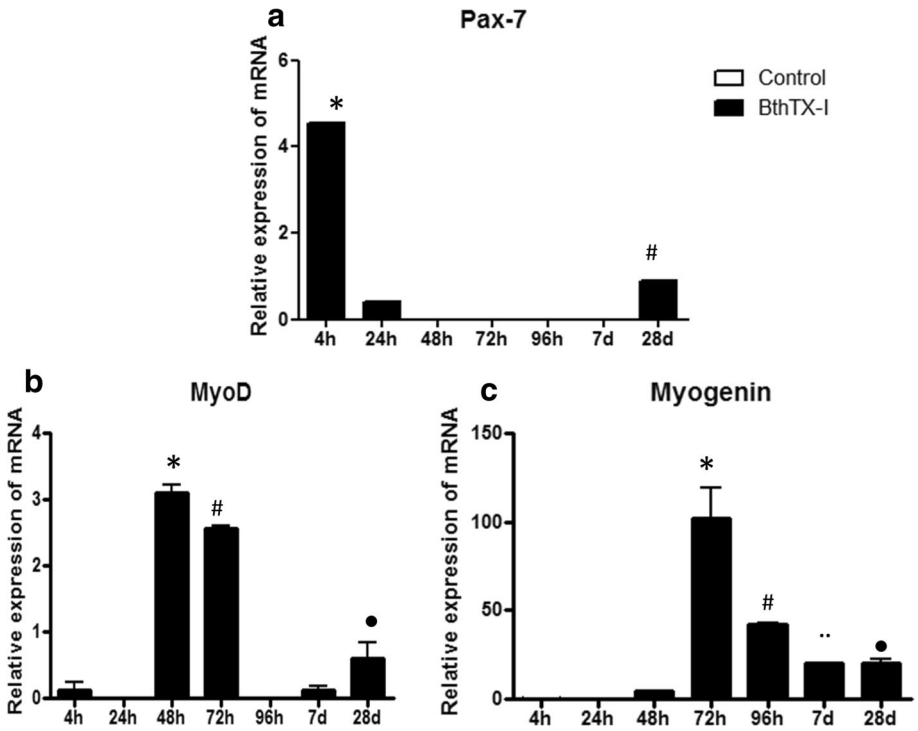

Fig. 4. mRNA expression for myogenic transcription factors in macerate muscle of BALB/c mice injected with BthTX-I. Cell suspensions were prepared from gastrocnemius muscle of BALB/c mice after 4, 24, 48, 72, 96 h, 7, and 28 days after injection of BthTX-I. The expression of the transcription factors was done by real-time PCR as described in "Materials and methods" section. The results were expressed as relative amount of cDNA using the β-actin as gene constitutive expression. $p < 0.05$. **a** PAX-7 mRNA expression**.** *$p < 0.05$ 4-h BthTX-I group compared with other groups post-BthTX-I; #$p < 0.05$ BthTX-I 28-day group compared with the other groups. **b** MyoD mRNA expression. *$p < 0.05$ BthTX-I 48-h group group compared with the other groups; #$p < 0.05$ BthTX-I 72-h group compared with the other groups; •$p < 0.05$ BthTX-I 28-day group compared with the other groups. **c** Myogenin mRNA expression. *$p < 0.05$ BthTX-I 72-h group compared with the other groups; #$p < 0.05$ BthTX-I 96-h group compared with the other groups; ¨ $p < 0.05$ BthTX-I 7-day group compared with the other groups; (•)$p < 0.05$ BthTX-I 28-day group compared with the other groups.

myotoxic activity of the toxin [11, 14, 43, 53]. These observations are in agreement with those described by Gutierrez et al. [54] that demonstrated the direct effect of a PLA_2 isolated from *Bothrops asper* venom on muscle fibers at the first few hours of toxin injection resulting in tissue necrosis. In addition, these authors verified intense influx of neutrophils and macrophages after 24 to 72 h after the toxin injection. At 7 days after BthTX-I injection, we verified an intense regenerative process, and on 28th day, almost complete muscle regeneration was verified, similarly to the data reported by Gutierrez et al. [55] when evaluating the effect of the bothropstoxin-II (BthTX-II), a myotoxic Asp-49 PLA_2 isolated from *B. jararacussu*.

Similar results were also showed by Teixeira et al. [56] in muscle damage induced by the injection of crude *B. asper* venom and its isolated myotoxin I. Furthermore, the data obtained in neutropenic mice in contrast with control mice, both injected with the venom or myotoxin I, showed that the neutrophils are involved in the phagocytosis of necrotic cells and may play a role in the recruitment and activation of macrophages and consequent muscle regenerating process.

Several studies have shown that distinct macrophage subsets modulate the skeletal muscle regeneration process in different experimental models [19, 23, 46]. Phagocytic macrophage $CD68^+$ is recruited to the inflammatory site, and in the course of the muscle repair, they are replaced by $CD206^+$ macrophages [57]. Similar balances in macrophage populations were also observed in the inflammatory reaction and regeneration that follows BthTX-I injection. In our experiments, we verified the time course of changes in macrophage populations, as observed by the presence of $F4/80^+/CD68^+$ cells and high expression of iNOS in cell suspension after 48 h followed by $F4/80^+/CD206^+$ cells, as well as the arginase expression in cellular suspensions obtained in latter times of the toxin injection. In agreement with these findings, the expression of inflammatory cytokines (IL-6 and TNF-α) was enhanced in cell suspension obtained at 48 h after BthTX-I injection

followed by the high expression of TGF-β at 96-h time point. Thus, as shown, we observed that myeloid cells at different stages of activation produced distinct soluble molecules, as cytokines, which are involved in distinct phases of the regenerating process [1]. In addition, our data show that the M2 macrophages are predominant in the later times post-BthTX-I injection coincidently with the regenerative phase observed in histological analysis. These findings are supported by published data that the elimination of cell debris in injured muscle coincides with the replacement of M1 macrophages to M2 profile, indicating that the phagocytosis of the necrotic cells promotes a switch in their phenotype to acquire an anti-inflammatory function [46]. These M2 macrophages are activated by Th2 cytokines and also secrete IL-4, IL-10, and TGF-β, which induces the synthesis and accumulation of extracellular matrix components [58].

Arnold and collaborators [46] using CXCR3$^{GFP/+}$ mouse demonstrated a predominant CX3CR1^{lo}/Ly6C^{+} cells exhibiting inflammatory profile in the muscle injury after 24 h of the NTX injection followed by the switch for CX3CR1^{ho}/Ly6C^{-} anti-inflammatory cells, which persist up to 7 days post-injury. The analysis of the cytokine expression of isolated Ly6C^{+} and Ly6C^{-} cells at 4 days after injury showed higher expression of IL-1β and lesser TNF-α in Ly6C^{+} than Ly6C^{-} cells. On the other hand, TGFβ and IL-10 transcripts were stronger in LyC6^{-} than Ly6C^{+} cells indicating that these populations exhibit distinct functional profiles. Furthermore, the authors demonstrated in the muscle that LyC6^{+} cells switch their phenotype to anti-inflammatory with the phagocytosis of cellular debris and consequent initiation of the regeneration process. Our results are in agreement with those finding, since we verified the close relation between the macrophage subsets (M1 and M2) and cytokine microenvironment throughout the different phases of process developed in the muscle injured after the K49-myotoxin injection.

Following the tissue injury, concomitant with the immune cell influx, the myogenesis is displayed by the activation of the myogenic cells through sequential expression of transcription factors and activation of genes that culminate with the tissue regeneration [59]. Our data demonstrate an upregulation of MyoD expression at 48–72 h followed by later expression of myogenin in cell suspension obtained from muscle tissue after BthTX-I injection. Our data are in agreement with other injury models, as the cardiotoxin injection, that demonstrated increased expression of MyoD after 2–3 days post-injury in mouse muscle followed by an enhancement of myogenin and other transcripts during the regeneration process [1, 60, 61].

The role of factors, as cytokines, released by distinct macrophage populations on the muscle regenerative process has been confirmed in different *in vivo* and *in vitro* experimental models, as example, the finding that conditioned media from J774 macrophage cultures are able to induce increased of MyoD expression in myoblasts as well as the expression of myogenin when added in muscle cell cultures at later phases of differentiation [1, 13]. Besides the effect of the TNF-α and IL-6 on the inflammatory reaction, several findings have demonstrated their direct effect on muscle cells. In this sense, it was showed elevated expression of TNF-α receptors by muscle cells in consequence the tissue damage and during the regenerative process. Moreover, TNF-α null mutants and TNF-α receptor mutants mice presented lower levels of MyoD and MEF-2 expression in muscle cells post-injury compared with wild-type mice [1, 14, 62, 63]. Furthermore, the addition of IL-6 to myoblasts in culture induces proliferation, but not fusion of muscle cells indicating the role of this cytokine in the muscle growth [1, 64]. We also verified increased expression of IL-6 and TNF-α at the first times of BthTX-I injection indicating the role of these cytokines in the acute inflammatory phase and also the initiation of the regenerative process as the MyoD expression by satellite cells.

Several models have been substantiating the relevance of M2 macrophages on the later muscle regenerative phases, as demonstrated by the diminished muscle repair, differentiation, and regeneration in a model of depletion of the late invading macrophage population post-injury [1]. In agreement with this, M2 macrophages (Arg^{high}/IL-4R^{+}/CD206^{+}) producing IL-10 and TGF-β that are prevalent in the regenerative muscle play a role in the deactivation of M1 macrophages and modulation of the muscle cell activation and differentiation [63]. TGF-β is implicated in the regeneration process influencing the activity of inflammatory cells in the damage tissue, interfering with the myogenic differentiation and also promoting the connective tissue formation [65]. Thus, in our data, we also verified that the increased expression of TGF-β was coincident with the prevalence of M2 macrophage population in the muscle tissue post-BthTX-I injection that was confirmed by the later mononuclear infiltration observed in the histological analysis at 72 and 96 h. In addition, we observed high expression of PAX-7 on cell suspension post-BthTX-I injection indicating the presence of satellite cells—precursor myogenic cells (MPCs) at quiescent state. At 48–72 h, a decreased PAX-7 expression was coincident with the enhancement of MyoD expression and the high expression of myogenin at 72–96 h that represents the

proliferating and differentiation phases of regeneration, as previously confirmed in distinct experimental models of muscle injury [66]. At 28 days after the BthTX-I injury, it was also verified the PAX-7 expression representing the presence of new quiescent satellite cells, as well as the expression of myogenin indicating the nascent muscle fibers and the restoration of the muscle tissue.

The effective muscle regeneration depends on sequential events triggered after the damage tissue including the development of the inflammation and its downregulation, restoration of the vascular tissue, and innervation associated with a synthesis of extracellular matrix components, which restore the muscle architecture [65, 67, 68]. Thus, the set of our results allow us to demonstrate that the tightly regulated interaction between the immune system and myogenesis process triggered by a K49-PLA_2 isolated from snake venom follows the normal patterns of regeneration process that ensures the success of tissue regeneration.

ACKNOWLEDGEMENTS

Priscila Andrade Ranéia e Silva received a fellowship from Coordenação de Aperfeiçoamento de Pessoal de Nível Superior (CAPES). We thank Dr. Jorge M.C. Ferreira-Jr. for his help in flow cytometry.

FUNDING INFORMATION

This study was supported by Conselho Nacional de Desenvolvimento Científico e Tecnológico (CNPq) (311915/2012-4; 309392/2015-2).

COMPLIANCE WITH ETHICAL STANDARDS

All applicable international, national, and/or institutional guidelines for the care and use of animals were followed. All procedures performed in studies involving animals were in accordance with the ethical standards of the institution or practice at which the studies were conducted.

REFERENCES

1. Tidball, J.G., and S.A. Villalta. 2010. Regulatory interactions between muscle and the immune system during muscle regeneration. *American Journal of Physiology. Regulatory, Integrative and Comparative Physiology* 298: R1173–R1187.
2. Gutiérrez, J.M. 2012. Improving antivenom availability and accessibility: science, technology, and beyond. *Toxicon* 60: 676–687.
3. Williams, D., J.M. Gutiérrez, R. Harrison, D.A. Warrell, J. White, K.D. Winkel, and P. Gopalakrishnakone. 2010. The Global Snake Bite Initiative: an antidote for snake bite. *Lancet* 375: 89–91.
4. Otero, R., J. Gutiérrez, M. Beatriz Mesa, E. Duque, O. Rodríguez, J. Luis Arango, et al. 2002. Complications of Bothrops, Porthidium, and Bothriechis snakebites in Colombia. A clinical and epidemiological study of 39 cases attended in a university hospital. *Toxicon* 40: 1107–1114.
5. Gutiérrez, J.M., T. Escalante, and A. Rucavado. 2009. Experimental pathophysiology of systemic alterations induced by Bothrops asper snake venom. *Toxicon* 54: 976–987.
6. Bjarnason, J.B., and J.W. Fox. 1994. Hemorrhagic metalloproteinases from snake venoms. *Pharmacology & Therapeutics* 62: 325–372.
7. Kamiguti, A.S., J.R. Slupsky, M. Zuzel, and C.R. Hay. 1994. Properties of fibrinogen cleaved by Jararhagin, a metalloproteinase from the venom of Bothrops jararaca. *Thrombosis and Haemostasis* 72: 244–249.
8. Kamiguti, A.S., C.R. Hay, R.D. Theakston, and M. Zuzel. 1996. Insights into the mechanism of haemorrhage caused by snake venom metalloproteinases. *Toxicon* 34: 627–642.
9. Gutiérrez, J.M., and C.L. Ownby. 2003. Skeletal muscle degeneration induced by venom phospholipases A2: insights into the mechanisms of local and systemic myotoxicity. *Toxicon* 42: 915–931.
10. Lomonte, B., Y. Angulo, and L. Calderón. 2003. An overview of lysine-49 phospholipase A2 myotoxins from crotalid snake venoms and their structural determinants of myotoxic action. *Toxicon* 42: 885–901.
11. Homsi-Brandeburgo, M.I., L.S. Queiroz, H. Santo-Neto, L. Rodrigues-Simioni, and J.R. Giglio. 1988. Fractionation of Bothrops jararacussu snake venom: partial chemical characterization and biological activity of bothropstoxin. *Toxicon* 26: 615–627.
12. Cintra, A.C., S. Marangoni, B. Oliveira, and J.R. Giglio. 1993. Bothropstoxin-I: amino acid sequence and function. *Journal of Protein Chemistry* 12: 57–64.
13. Rodrigues-Simioni, L., N. Borgese, and B. Ceccarelli. 1983. The effects of Bothrops jararacussu venom and its components on frog nerve-muscle preparation. *Neuroscience* 10: 475–489.
14. Heluany, N.F., M.I. Homsi-Brandeburgo, J.R. Giglio, J. Prado-Franceschi, and L. Rodrigues-Simioni. 1992. Effects induced by bothropstoxin, a component from Bothrops jararacussu snake venom, on mouse and chick muscle preparations. *Toxicon* 30: 1203–1210.
15. Johnson, E.K., and C.L. Ownby. 1994. The role of extracellular ions in the pathogenesis of myonecrosis induced by a myotoxin isolated from broad-banded copperhead (Agkistrodon contortrix laticinctus) venom. *Comparative Biochemistry and Physiology. Pharmacology, Toxicology and Endocrinology* 107: 359–366.
16. Incerpi, S., P. de Vito, P. Luly, and S. Rufini. 1995. Effect of ammodytin L from Vipera ammodytes on L-6 cells from rat skeletal muscle. *Biochimica et Biophysica Acta* 1268: 137–142.
17. Cintra-Francischinelli, M., P. Pizzo, L. Rodrigues-Simioni, L.A. Ponce-Soto, O. Rossetto, B. Lomonte, J.M. Gutiérrez, T. Pozzan, and C. Montecucco. 2009. Calcium imaging of muscle cells treated with snake myotoxins reveals toxin synergism and presence of acceptors. *Cellular and Molecular Life Sciences* 66: 1718–1728.
18. Soares, A.M., W.P. Sestito, S. Marcussi, R.G. Stábeli, S.H. Andrião-Escarso, O.A. Cunha, et al. 2004. Alkylation of myotoxic phospholipases A2 in Bothrops moojeni venom: a promising approach to an enhanced antivenom production. *The International Journal of Biochemistry & Cell Biology* 36: 258–270.

19. Doin-Silva, R., V. Baranauskas, L. Rodrigues-Simioni, and M.A. da Cruz-Höfling. 2009. The ability of low level laser therapy to prevent muscle tissue damage induced by snake venom. *Photochemistry and Photobiology* 85: 63–69.
20. Schiaffino, S., C. Mammucari, and M. Sandri. 2008. The role of autophagy in neonatal tissues: just a response to amino acid starvation? *Autophagy* 4: 727–730.
21. Saclier, M., S. Cuvellier, M. Magnan, R. Mounier, and B. Chazaud. 2013. Monocyte/macrophage interactions with myogenic precursor cells during skeletal muscle regeneration. *The FEBS Journal* 280: 4118–4130.
22. Gordon, S., and F.O. Martinez. 2010. Alternative activation of macrophages: mechanism and functions. *Immunity* 32: 593–604.
23. Gordon, S., and P.R. Taylor. 2005. Monocyte and macrophage heterogeneity. *Nature Reviews. Immunology* 5: 953–964.
24. Mantovani, A., S. Sozzani, M. Locati, P. Allavena, and A. Sica. 2002. Macrophage polarization: tumor-associated macrophages as a paradigm for polarized M2 mononuclear phagocytes. *Trends in Immunology* 23: 549–555.
25. Mantovani, A., A. Sica, S. Sozzani, P. Allavena, A. Vecchi, and M. Locati. 2004. The chemokine system in diverse forms of macrophage activation and polarization. *Trends in Immunology* 25: 677–686.
26. Wehling-Henricks, M., J.J. Lee, and J.G. Tidball. 2004. Prednisolone decreases cellular adhesion molecules required for inflammatory cell infiltration in dystrophin-deficient skeletal muscle. *Neuromuscular Disorders* 14: 483–490.
27. Martinez, F.O., and S. Gordon. 2014. The M1 and M2 paradigm of macrophage activation: time for reassessment. *F1000Prime Rep* 6: 13.
28. St Pierre, B.A., and J.G. Tidball. 1994. Differential response of macrophage subpopulations to soleus muscle reloading after rat hindlimb suspension. *Journal of Applied Physiology (Bethesda, MD: 1985)* 77: 290–297.
29. Tidball, J.G., E. Berchenko, and J. Frenette. 1999. Macrophage invasion does not contribute to muscle membrane injury during inflammation. *Journal of Leukocyte Biology* 65: 492–498.
30. Schwartz, YSh, and A.V. Svistelnik. 2012. Functional phenotypes of macrophages and the M1-M2 polarization concept. Part I. Proinflammatory phenotype. *Biochemistry (Moscow)* 77: 246–260.
31. Moura-da-Silva, A.M., H. Desmond, G. Laing, and R.D. Theakston. 1991. Isolation and comparison of myotoxins isolated from venoms of different species of Bothrops snakes. *Toxicon* 29: 713–723.
32. Overbergh, L., D. Valckx, M. Waer, and C. Mathieu. 1999. Quantification of murine cytokine mRNAs using real time quantitative reverse transcriptase PCR. *Cytokine* 11: 305–312.
33. Cornelison, D.D., and B.J. Wold. 1997. Single-cell analysis of regulatory gene expression in quiescent and activated mouse skeletal muscle satellite cells. *Developmental Biology* 191: 270–283.
34. Murray, P.J., J.E. Allen, S.K. Biswas, E.A. Fisher, D.W. Gilroy, S. Goerdt, S. Gordon, J.A. Hamilton, L.B. Ivashkiv, T. Lawrence, M. Locati, A. Mantovani, F.O. Martinez, J.L. Mege, D.M. Mosser, G. Natoli, J.P. Saeij, J.L. Schultze, K.A. Shirey, A. Sica, J. Suttles, I. Udalova, J.A. van Ginderachter, S.N. Vogel, and T.A. Wynn. 2014. Macrophage activation and polarization: nomenclature and experimental guidelines. *Immunity* 41: 14–20.
35. Munder, M., K. Eichmann, J.M. Morán, F. Centeno, G. Soler, and M. Modolell. 1999. Th1/Th2-regulated expression of arginase isoforms in murine macrophages and dendritic cells. *Journal of Immunology* 163: 3771–3777.
36. Arce, V., F. Brenes, and J.M. Gutiérrez. 1991. Degenerative and regenerative changes in murine skeletal muscle after injection of venom from the snake Bothrops asper: a histochemical and immunocytochemical study. *International Journal of Experimental Pathology* 72: 211–226.
37. Ciciliot, S., and S. Schiaffino. 2010. Regeneration of mammalian skeletal muscle. Basic mechanisms and clinical implications. *Current Pharmaceutical Design* 16: 906–914.
38. Le Grand, F., and M.A. Rudnicki. 2007. Skeletal muscle satellite cells and adult myogenesis. *Current Opinion in Cell Biology* 19: 628–633.
39. Jung, S., J. Aliberti, P. Graemmel, M.J. Sunshine, G.W. Kreutzberg, A. Sher, and D.R. Littman. 2000. Analysis of fractalkine receptor CX(3)CR1 function by targeted deletion and green fluorescent protein reporter gene insertion. *Molecular and Cellular Biology* 20: 4106–4114.
40. Choi, J., M.L. Costa, C.S. Mermelstein, C. Chagas, S. Holtzer, and H. Holtzer. 1990. MyoD converts primary dermal fibroblasts, chondroblasts, smooth muscle, and retinal pigmented epithelial cells into striated mononucleated myoblasts and multinucleated myotubes. *Proceedings of the National Academy of Sciences of the United States of America* 87: 7988–7992.
41. Kassar-Duchossoy, L., B. Gayraud-Morel, D. Gomès, D. Rocancourt, M. Buckingham, V. Shinin, and S. Tajbakhsh. 2004. Mrf4 determines skeletal muscle identity in Myf5:Myod double-mutant mice. *Nature* 431: 466–471.
42. Kamiguti, A.S., R.D. Theakston, H. Desmond, and R.A. Hutton. 1991. Systemic haemorrhage in rats induced by a haemorrhagic fraction from Bothrops jararaca venom. *Toxicon* 29: 1097–1105.
43. Paine, M.J., H.P. Desmond, R.D. Theakston, and J.M. Crampton. 1992. Purification, cloning, and molecular characterization of a high molecular weight hemorrhagic metalloprotease, jararhagin, from Bothrops jararaca venom. Insights into the disintegrin gene family. *The Journal of Biological Chemistry* 267: 22869–22876.
44. Moura-da-Silva, A.M., R.D. Theakston, and J.M. Crampton. 1996. Evolution of disintegrin cysteine-rich and mammalian matrix-degrading metalloproteinases: gene duplication and divergence of a common ancestor rather than convergent evolution. *Journal of Molecular Evolution* 43: 263–269.
45. Moura-da-Silva, A.M., O.H. Ramos, C. Baldo, S. Niland, U. Hansen, J.S. Ventura, et al. 2008. Collagen binding is a key factor for the hemorrhagic activity of snake venom metalloproteinases. *Biochimie* 90: 484–492.
46. Arnold, L., A. Henry, F. Poron, Y. Baba-Amer, N. van Rooijen, A. Plonquet, R.K. Gherardi, and B. Chazaud. 2007. Inflammatory monocytes recruited after skeletal muscle injury switch into antiinflammatory macrophages to support myogenesis. *The Journal of Experimental Medicine* 204: 1057–1069.
47. Kehl, L.J., T.M. Trempe, and K.M. Hargreaves. 2000. A new animal model for assessing mechanisms and management of muscle hyperalgesia. *Pain* 85: 333–343.
48. Pinniger, G.J., T. Lavin, and A.J. Bakker. 2012. Skeletal muscle weakness caused by carrageenan-induced inflammation. *Muscle & Nerve* 46: 413–420.
49. Radhakrishnan, R., S.A. Moore, and K.A. Sluka. 2003. Unilateral carrageenan injection into muscle or joint induces chronic bilateral hyperalgesia in rats. *Pain* 104: 567–577.
50. Ainsworth, L., K. Budelier, M. Clinesmith, A. Fiedler, R. Landstrom, B.J. Leeper, L.A. Moeller, S. Mutch, K. O Dell, J. Ross, R. Radhakrishnan, and K.A. Sluka. 2006. Transcutaneous electrical nerve stimulation (TENS) reduces chronic hyperalgesia induced by muscle inflammation. *Pain* 120: 182–187.
51. Loram, L.C., A. Fuller, L.G. Fick, T. Cartmell, S. Poole, and D. Mitchell. 2007. Cytokine profiles during carrageenan-induced inflammatory hyperalgesia in rat muscle and hind paw. *The Journal of Pain* 8: 127–136.

52. Hardy, D., A. Besnard, M. Latil, G. Jouvion, D. Briand, C. Thépenier, Q. Pascal, A. Guguin, B. Gayraud-Morel, J.M. Cavaillon, S. Tajbakhsh, P. Rocheteau, and F. Chrétien. 2016. Comparative study of injury models for studying muscle regeneration in mice. *PLoS One* 11: e0147198.
53. Rodrigues-Simioni, L., J. Prado-Franceschi, A.C. Cintra, J.R. Giglio, M.S. Jiang, and J.E. Fletcher. 1995. No role for enzymatic activity or dantrolene-sensitive Ca2+ stores in the muscular effects of bothropstoxin, a Lys49 phospholipase A2 myotoxin. *Toxicon* 33: 1479–1489.
54. Gutiérrez, J.M., V. Arce, F. Brenes, and F. Chaves. 1990. Changes in myofibrillar components after skeletal muscle necrosis induced by a myotoxin isolated from the venom of the snake Bothrops asper. *Experimental and Molecular Pathology* 52: 25–36.
55. Gutiérrez, J.M., J. Núñez, C. Díaz, A.C. Cintra, M.I. Homsi-Brandeburgo, and J.R. Giglio. 1991. Skeletal muscle degeneration and regeneration after injection of bothropstoxin-II, a phospholipase A2 isolated from the venom of the snake Bothrops jararacussu. *Experimental and Molecular Pathology* 55: 217–229.
56. Teixeira, C.F., S.R. Zamunér, J.P. Zuliani, C.M. Fernandes, M.A. Cruz-Hofling, I. Fernandes, et al. 2003. Neutrophils do not contribute to local tissue damage, but play a key role in skeletal muscle regeneration, in mice injected with Bothrops asper snake venom. *Muscle & Nerve* 28: 449–459.
57. Villalta, S.A., H.X. Nguyen, B. Deng, T. Gotoh, and J.G. Tidball. 2009. Shifts in macrophage phenotypes and macrophage competition for arginine metabolism affect the severity of muscle pathology in muscular dystrophy. *Human Molecular Genetics* 18: 482–496.
58. Gordon, S. 2003. Alternative activation of macrophages. *Nature Reviews. Immunology* 3: 23–35.
59. Kauhanen, S., A. Salmi, K. von Boguslawski, S. Asko-Seljavaara, and I. Leivo. 2003. Satellite cell proliferation, reinnervation, and revascularization in human free microvascular muscle flaps. *The Journal of Surgical Research* 115: 191–199.
60. Couteaux, R., J.C. Mira, and A. d'Albis. 1988. Regeneration of muscles after cardiotoxin injury. I. Cytological aspects. *Biology of the Cell* 62: 171–182.
61. Wehling-Henricks, M., M.C. Jordan, T. Gotoh, W.W. Grody, K.P. Roos, and J.G. Tidball. 2010. Arginine metabolism by macrophages promotes cardiac and muscle fibrosis in mdx muscular dystrophy. *PLoS One* 5: e10763.
62. Warren, G.L., T. Hulderman, N. Jensen, M. McKinstry, M. Mishra, M.I. Luster, et al. 2002. Physiological role of tumor necrosis factor alpha in traumatic muscle injury. *The FASEB Journal* 16: 1630–1632.
63. Kharraz, Y., J. Guerra, C.J. Mann, A.L. Serrano, and P. Muñoz-Cánoves. 2013. Macrophage plasticity and the role of inflammation in skeletal muscle repair. *Mediators of Inflammation* 2013: 491497.
64. Serrano, A.L., B. Baeza-Raja, E. Perdiguero, M. Jardí, and P. Muñoz-Cánoves. 2008. Interleukin-6 is an essential regulator of satellite cell-mediated skeletal muscle hypertrophy. *Cell Metabolism* 7: 33–44.
65. Delaney, K., P. Kasprzycka, M.A. Ciemerych, and M. Zimowska. 2017. The role of TGF-β1 during skeletal muscle regeneration. *Cell Biology International* 41: 706–715.
66. Tidball, J.G. 2017. Regulation of muscle growth and regeneration by the immune system. *Nature Reviews. Immunology* 17: 165–178.
67. Järvinen, T.A., T.L. Järvinen, M. Kääriäinen, H. Kalimo, and M. Järvinen. 2005. Muscle injuries: biology and treatment. *The American Journal of Sports Medicine* 33: 745–764.
68. Tidball, J.G. 2005. Inflammatory processes in muscle injury and repair. *American Journal of Physiology. Regulatory, Integrative and Comparative Physiology* 288: R345–R353.